Seasonal drought stress in the Amazon: Reconciling models and observations

I. T. Baker,[1] L. Prihodko,[2] A. S. Denning,[1] M. Goulden,[3] S. Miller,[4] and H. R. da Rocha[5]

[1]   The Amazon Basin is crucial to global circulatory and carbon patterns due to the large areal extent and large flux magnitude. Biogeophysical models have had difficulty reproducing the annual cycle of net ecosystem exchange (NEE) of carbon in some regions of the Amazon, generally simulating uptake during the wet season and efflux during seasonal drought. In reality, the opposite occurs. Observational and modeling studies have identified several mechanisms that explain the observed annual cycle, including: (1) deep soil columns that can store large water amount, (2) the ability of deep roots to access moisture at depth when near-surface soil dries during annual drought, (3) movement of water in the soil via hydraulic redistribution, allowing for more efficient uptake of water during the wet season, and moistening of near-surface soil during the annual drought, and (4) photosynthetic response to elevated light levels as cloudiness decreases during the dry season. We incorporate these mechanisms into the third version of the Simple Biosphere model (SiB3) both singly and collectively, and confront the results with observations. For the forest to maintain function through seasonal drought, there must be sufficient water storage in the soil to sustain transpiration through the dry season in addition to the ability of the roots to access the stored water. We find that individually, none of these mechanisms by themselves produces a simulation of the annual cycle of NEE that matches the observed. When these mechanisms are combined into the model, NEE follows the general trend of the observations, showing efflux during the wet season and uptake during seasonal drought.

Citation: Baker, I. T., L. Prihodko, A. S. Denning, M. Goulden, S. Miller, and H. R. da Rocha (2008), Seasonal drought stress in the Amazon: Reconciling models and observations, *J. Geophys. Res.*, *113*, G00B01, doi:10.1029/2007JG000644.

1.   Introduction

[2]   Changes in the biophysical state of the Amazon rain forest exert a strong influence on global climate through associated changes in carbon and hydrological cycles [*Avissar and Werth*, 2004; *Zeng et al.*, 2005; *Marengo and Nobre*, 2001; *Kleidon and Heimann*, 1999]. Perturbations to these cycles, for example from drought, deforestation, and ENSO events, have a strong influence because of the sheer geographical size of the region (5.8×10^6 km^2 [*Salati and Vose*, 1984]), the role it plays in regional meteorology [*Nobre et al.*, 1991] and the magnitude of the carbon stored there [*Houghton et al.*, 2001]. Inversion studies have shown Tropical America to be a small source of CO_2 to the atmosphere [*Gurney et al.*, 2002; *Stephens et al.*, 2007], although the interannual variability is large [*Bousquet et al.*, 2000]. However, there is much we still don't understand about carbon and hydrological cycles in the Amazon, and this ambiguity leads to uncertainty in projections of future climate change [*Magrin et al.*, 2007; *Cox et al.*, 2000; *Friedlingstein et al.*, 2001].

[3]   Observational campaigns and concerted modeling efforts assist in quantifying impacts of the Amazon Rain forest on regional and global carbon and water cycles [*Andreae et al.*, 2002; *Avissar et al.*, 2002; *Keller et al.*, 2004]. However, results are not always in agreement [i.e., *Huete et al.*, 2006; *Lee et al.*, 2005; *Ichii et al.*, 2007]. To accurately characterize the carbon dynamics across vegetation and moisture gradients in Amazonia will require cooperation between observational and modeling studies to achieve understanding of the biophysics that force fluxes in the region.

[4]   The driving climatic forcing in the region is precipitation amount and temporal distribution. Total annual precipitation and the length of dry season, usually defined as number of months with less than 100 mm precipitation, play a large role in vegetation distribution and fluxes of energy, water and carbon [*Keller et al.*, 2004; *Goulden et al.*, 2004; *Saleska et al.*, 2003; *Ichii et al.*, 2007]. The seasonality of surface-atmosphere fluxes are further controlled by

[1]Atmospheric Science, Colorado State University, Fort Collins, Colorado, USA.
[2]Natural Resources Ecology Laboratory, Colorado State University, Fort Collins, Colorado, USA.
[3]Department of Earth System Science, Ecology, and Evolutionary Biology, University of California, Irvine, California, USA.
[4]Atmospheric Sciences Research Center, State University of New York, Albany, New York, USA.
[5]Instituto de Astronomica, Geofisica e Ciencias Atmosfericas, Universidade de São Paulo, São Paulo, Brazil.
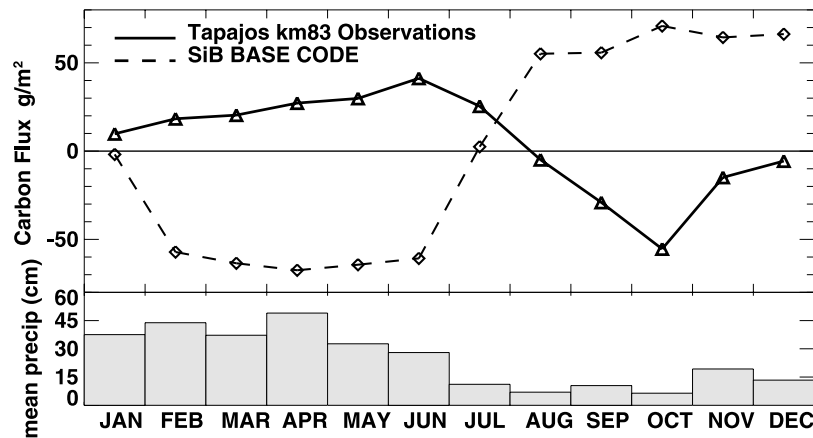
Figure 1. Average monthly net ecosystem exchange (NEE) of carbon in g m^2 at Tapajos National Forest km83 site, years 2001–2003. Observed flux is shown as solid line; SiB3 simulation is shown as dashed line. Mean monthly precipitation in cm is shown below for reference. Positive values indicate efflux into the atmosphere, and negative values indicate uptake by the biosphere.

topography, vegetation type, root depth, depth of soil and soil type. The carbon dynamics in the region are a function of carbon uptake by photosynthesis and release by respiration, with additional components of storage in soil and biomass and carbon export via runoff. Amazonia contains between 10 and 15% of the total global biomass [*Houghton et al.*, 2000]. A large fraction of the region consists of closed-canopy broadleaf evergreen forest, gradating to savanna (cerrado) in regions with less precipitation, although the cerrado is generally outside of the hydrogeographic basin of the Amazon River.

[5] The interaction between the wet/dry seasons and the annual cycle of CO$_2$ uptake/efflux is not consistent across the Amazon Basin; *Keller et al.* [2004] report observations of carbon uptake during the wet season at locations in Jaru Reserve and Fazenda Maracai, while several sites in the Tapajos National Forest report uptake during the dry season [*Saleska et al.*, 2003; *Goulden et al.*, 2004].

[6] *Saleska et al.* [2003] have shown that multiple ecosystem models are almost exactly out-of-phase with the observed annual NEE cycle in the seasonally dry Tapajos region. For example, Figure 1 shows observed and modeled average annual cycle of NEE for the years 2001–2003 using the Simple Biosphere model, version 3 (SiB3) [*Sellers et al.*, 1986, 1996a; *Baker et al.*, 2007]. Comparing our Figure 1 to Figure 3 of *Saleska et al.* [2003], the results are similar; SiB3 simulates CO$_2$ uptake during the wet season, and efflux during seasonal drought, as the model vegetation experiences stress due to declining soil moisture. The observations show exactly the opposite: efflux during the wet season, and uptake of carbon during the relative dry period of August–December. In SiB3, soil moisture and the ability of the roots to access water in the soil are the driving mechanisms that determine the annual cycle of NEE. When the soil is moist, carbon uptake is unstressed, and as the model soil desiccates in the dry season, the photosynthetic uptake is restricted. Model respiration is reasonably constant throughout the year, with the result that as photosynthesis wanes during the dry season, a net efflux of carbon to the atmosphere is produced. By identifying the mechanisms that operate in the real world and modifying model physics

to incorporate them, we have an opportunity to improve model simulations and deepen our understanding of the system.

[7] What responses has the local vegetation evolved to cope with seasonal drought? Up to half of the closed canopy forest in Brazilian Amazonia is able to access water in the soil at depths of 15 m or more, with roots that extend deep into the soil [*Nepstad et al.*, 1994; *Jipp et al.*, 1998]. Using a water-balance approach, *Nepstad et al.* [1994] estimated that greater than 75% of the water extracted from the soil during the 1992 dry season at a forest in the Brazilian state of Para came from a depth greater than 2 m. Roots were most abundant near the surface, but up to 10% of the total rooting mass was at depths between 4 and 10 m. *Kleidon and Heimann* [1999] found that the inclusion of deep roots in climate models resulted in a better representation of seasonal air temperature. *Ichii et al.* [2007] found that rooting depth was critical for reconciling modeled Gross Primary Productivity (GPP) with satellite observations. Roots can act as conduits to move water within the soil as well: *Oliveira et al.* [2005] found that roots in three species of trees in the Tapajos National Forest had the ability to move water both upward and downward in the soil in response to moisture potential gradients. Briefly, when stomates are closed at night moisture can move through roots from moist regions of soil to areas of large saturation deficit. This is referred to as hydraulic redistribution (HR). During the dry season, near-surface soil layers are recharged with moisture from the deep soil, and during the wet season roots can supplement infiltration to make deep soil recharge more efficient. *da Rocha et al.* [2004] observed apparent recharge of surface soil layers at the KM83 site in the Tapajos region either through HR or the capillary action of the soil (observed at other Amazonian sites [*Romero-Saltos et al.*, 2005]). *Lee et al.* [2005] incorporated the HR mechanism into the Community Land Model (CLM) coupled to the Community Atmosphere Model, Version 2 (CAM2) and found that HR elevated soil moisture at all levels of the soil when compared to a control run. The control run had less photosynthesis than the HR simulation in all months, however the HR run still had 50% less

photosynthesis during the dry season when compared to the wet season.

[8] Studies using satellite-based observations of forest greenness have postulated that there is actually an increase in photosynthesis during the dry season, as forests respond to higher light levels in the absence of cloudiness. Using Enhanced Vegetation Index (EVI) data from the Moderate Resolution Imaging Spectroradiometer (MODIS), *Huete et al.* [2006] noted a 25% green-up across large portions of Amazon forest during the dry season. This result suggests that light response may play as large or larger role than phenology or rainfall variability in determining annual cycle of carbon flux. In grasslands, EVI was found to decrease during the dry season [*Huete et al.*, 2006; *Saleska et al.*, 2007] in contrast to the increase found in forests; this suggests that rooting depth or hydraulic redistribution associated with deep roots plays a significant role in the dry season green up, as grasses do not have the deep root density found in forests. The conceptual model that emerges, then, is one where soil depth and the ability of roots to utilize stored water is crucial to the ability of the forest to maintain function through annual drought that may last 6 months or more. The deep soil provides a reservoir to store rainfall from the wet season for use during the dry months of the year. Hydraulic redistribution by roots can enhance the ability of the soil to recharge moisture via infiltration, and can moisten near-surface layers by moving water upward against gravity during the dry season. The soil hydraulics and root function provide a framework where photosynthesis does not experience large-scale annual stress, and more subtle mechanisms of photosynthetic response to light and of respiration response to slight changes in soil and litter moisture levels interact to provide the observed annual cycle of NEE.

[9] This study focused on the CO_2 flux at the km83 tower in the Tapajos National Forest [*Goulden et al.*, 2004; *Miller et al.*, 2004]. We simulated 3 years of fluxes between the atmosphere and terrestrial biosphere (emphasizing net ecosystem exchange of Carbon, or NEE) using the simple biosphere model (SiB3) [*Sellers et al.*, 1986, 1996a; *Baker et al.*, 2003] and then, by identifying possible mechanisms not present in the model, we modify the model code and rerun the simulations, resulting in model carbon flux that is more realistic when compared to the observed flux. By confronting model simulations with observations, we can identify mechanisms that are incorrectly treated, and by noting the changes in model flux with inclusion of new mechanisms or modification of existing ones, we can make inferences about biophysical behavior in this region.

2. Methods

2.1. Site Description

[10] The Tapajos National Forest km83 site is described in detail elsewhere [*Goulden et al.*, 2004; *da Rocha et al.*, 2004; *Miller et al.*, 2004]; however, a brief description is given here to provide details specific to this paper. The vegetation is closed canopy, mostly evergreen, with a few deciduous species. The tower is located in a region of minimal topographic relief; within several kilometers, elevation change is on the order of 10 m. The region was selectively logged in September 2001. However, the amount

of total biomass removed was small (5%), and seasonal cycles of carbon flux as measured by the tower were not altered. Soil texture and carbon content varies across the site and are described in detail by *Silver et al.* [2000]. For the years 2001–2003, the average precipitation was 1658 mm, with a maximum of 1764 mm in 2003, and a minimum of 1559 mm in 2002. The dry season extended approximately from July through December, although there were individual months in this period with precipitation slightly in excess of 100 mm (December 2002, September 2003, November–December 2003) and over 200 mm of rain in November 2002. The precipitation recorded by the gauges for 2001–2003 is approximately 15% lower than what is reported in the region by the Global Precipitation Climatology Product (GPCP) [*Adler et al.*, 2003]. However, we believe that there is not a seasonal bias, and so have chosen not to artificially manipulate the precipitation data.

2.2. Model Description

[11] The Simple Biosphere model (SiB) is a land-surface parameterization scheme originally used to simulate biophysical processes in climate models [*Sellers et al.*, 1986], but later adapted to include ecosystem metabolism [*Sellers et al.*, 1996a; *Denning et al.*, 1996]. SiB is a model that is useful to meteorologists for its ability to simulate exchanges of mass, energy and momentum between the atmosphere and terrestrial biosphere, and useful to ecologists for its ability to do so in a process-based framework that allows for simulation of explicit biophysical mechanisms. The parameterization of photosynthetic carbon assimilation is based on enzyme kinetics originally developed by *Farquhar et al.* [1980], and is linked to stomatal conductance and thence to the surface energy budget and atmospheric climate [*Collatz et al.*, 1991, 1992; *Sellers et al.*, 1996a; *Randall et al.*, 1996]. The soil representation is similar to that of CLM [*Dai et al.* 2003], with 10 soil layers and an initial soil column depth of 3.5 m. SiB has been updated to include prognostic calculation of temperature, moisture, and trace gases in the canopy air space, and the model has been evaluated against eddy covariance measurements at a number of sites [*Baker et al.*, 2003; *Hanan et al.*, 2005; *Vidale and Stöckli*, 2005]. We refer to this base version of the code as SiB3.

[12] We used half-hourly, gap-filled observations of air temperature, pressure, humidity, wind speed, radiation and precipitation from the km83 site [*Miller et al.*, 2004; *da Rocha et al.*, 2004; *Goulden et al.*, 2004] to drive the model for the years 2001 through 2003. Model parameters are determined using a combination of satellite data, literature values and standard SiB parameters [*Sellers et al.*, 1996b]. The annual cycle of Normalized Difference Vegetation Index (NDVI) collected over the km83 site is badly contaminated by clouds for all satellite products. Since there were no leaf area index measurements available for the site, it was not possible to determine whether there was a measurable phenological change (though one has been hypothesized by *Goulden et al.* [2004]). Thus a constant value of NDVI equal to 0.8, derived from the Global Inventory Monitoring and Modeling Study (GIMMSg) data set [*Tucker et al.*, 2005], was used in the parameterization of the model. Soil texture, used by SiB3 to determine physical and hydrological characteristics of the soil, was set as sandy

clay (52% sand and 46% clay) and was based on observations made in the area [*Silver et al.*, 2000]. Root distribution follows *Jackson et al.* [1996] for broadleaf evergreen forest, and every soil layer, even at depth, has a nonzero root fraction.

[13] The coupling between photosynthesis/transpiration and soil processes is achieved by an initial calculation of soil moisture stress on photosynthesis, followed by an algorithm for removing water from the soil once transpiration has been calculated. The calculation of water stress is commonly linked directly to root density as follows:

$$waterstress = \sum_{i=1}^{nsoil} \left(\frac{1 - \frac{\theta_{wp}}{\theta_i}}{1 - \frac{\theta_{wp}}{\theta_{fc}}} \right)(rootf_i), \qquad (1)$$

where *nsoil* is the number of soil layers, θ_{wp} is volumetric soil water fraction at wilt point, θ_{fc} is volumetric soil water fraction at field capacity, θ_i is volumetric soil water fraction of soil layer *i*, and $rootf_i$ is root fraction in soil layer *i*. Soil water stress on photosynthesis is calculated using the assumption that soil containing water at or above field capacity imposes no stress on photosynthesis, while soil at or below wilt point (defined as a moisture potential of −150 m) will result in almost complete loss of carboxylation capacity and attendant stomatal closure. The contribution of each model soil layer to overall stress is normalized by root fraction. Removal of water from the soil by transpiration follows the same process. The base SiB3 case, shown in Figure 1, shows the model NEE cycle obtained using this representation of soil water stress and water removal mechanisms.

3. Analysis

[14] We implemented the evolutionary responses/biophysical mechanisms described in the introduction into SiB3 individually, to gauge model response. The primary metric for evaluation of model performance is Net Primary Production (NPP), defined as autotrophic respiration from canopy vegetation (not roots) less gross photosynthesis. On monthly timescales, net ecosystem exchange (NEE) can be defined as $R_{soil} - $ NPP, where R_{soil} is defined as heterotrophic respiration in the soil. We follow the convention that positive NEE implies flux into the atmosphere, while negative NEE depicts carbon flux into the terrestrial biosphere. The individual sensitivity studies are as follows.

3.1. Soil Water Stress/Rooting Distribution (SiB3-SR)

[15] Total soil column depth (3.5 m) is unchanged, but soil water stress on photosynthesis is modified to relax the direct coupling to root fraction in each soil layer. Soil moisture deficit below field capacity for each layer is aggregated and a total-column stress amount is determined as follows:

$$waterstress = \frac{(1 + wssp)\frac{w_{column}}{w_{max}}}{wssp + \frac{w_{column}}{w_{max}}}, \qquad (2)$$

where w_{column} is water in the column in excess of wilt point (kg), w_{max} is maximum possible excess of water in the column (field capacity less wilt point; kilograms), and *wssp* is a water stress curvature parameter (currently chosen as 0.2).

[16] Stress on the whole ecosystem is thus parameterized as a function of plant available water within the total column, independent of root distribution. The new formulation provides a more gradual response to stress in the model, marked by a smooth transition between nonstressed and stressed regimes. For water removal by transpiration, an 'apparent' root fraction is determined for each soil layer depending on actual root fraction and moisture content of the layer.

$$rootr_i = \left(\frac{1 - \frac{\theta_{wp}}{\theta_i}}{1 - \frac{\theta_{wp}}{\theta_{fc}}} \right)(rootf_i). \qquad (3)$$

The apparent root fraction ($rootr_i$) is summed over the column, and each layer is normalized so that $rootr_{column}$ is unity. The apparent root fraction can be higher or lower than the initial root fraction ($rootf_i$) on the basis of water content in the individual layer convolved with the moisture distribution within the column. This apparent root fraction is consistent with the observed ability of deep roots to carry large amount of water as reported by *Jipp et al.* [1998] or *Nepstad et al.* [1994], and is mentioned by *Lee et al.* [2005] as well.

3.2. Hydraulic Redistribution (SiB3-HR)

[17] Following *Lee et al.* [2005] we incorporated a hydraulic redistribution term into the Darcy's Law equations used to calculate vertical movement of soil water. Coding follows *Ryel et al.* [2002] and root conductivity values are taken directly from *Lee et al.* [2005]. The HR modifications allow soil water to move downward more efficiently during periods of rain, and restore water to near-surface layers during dry periods. Total soil column depth remains 3.5 m.

3.3. Soil Modification (SiB3-DS, or Deep Soil)

[18] Similar to case SiB3-SR, but we increase the total soil depth to 10 m. The number of layers (10) in the model is unchanged, but each layer is increased in thickness. This treatment differs from the HR case both in the total depth of the 'reservoir' for water storage and because no water is redistributed between layers (other than basic infiltration or downgradient flow), therefore the storage dynamics are different. An additional modification to the soil in the DS case is the saturation fraction for maximum soil respiration. Following *Raich et al.* [1991], the relative rate of heterotrophic respiration is tied to soil moisture amount, dependent on type of soil. We found that the optimum soil moisture for respiration at km83 was too low in the model, so that there was almost no response of heterotrophic respiration to soil moisture. Soil respiration was dependent only upon soil temperature. However, observations showed that the annual average volumetric soil moisture at 10 cm was 0.34 m^3 m^{-3}, giving a percent of saturation of approximately 75–80%. By increasing the optimum soil moisture value for heterotrophic respiration to 75%, we were able to induce a respiration response to modeled annual cycles of soil moisture.
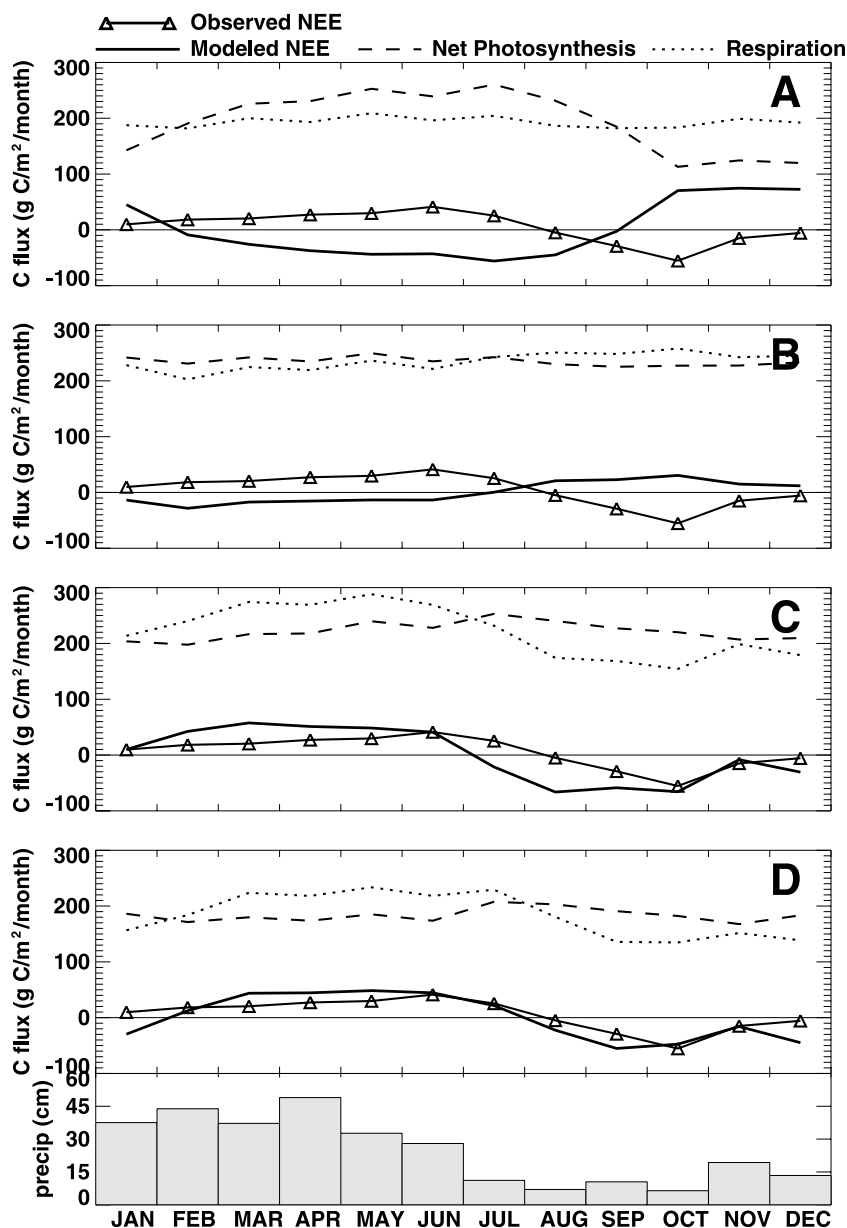
Figure 2. Average monthly photosynthesis (dashed line), respiration (dotted line), and NEE (solid line) for four SiB3 simulations. (a) Relaxed root stress calculation (SiB3-SR), (b) hydraulic Redistribution (SiB3-HR), (c) soil depth/respiration modification (SiB3-DS), and (d) combination of the four mechanism runs. Mean monthly precipitation in centimeters is shown at the bottom for reference. Positive NEE values indicate efflux into the atmosphere, and negative values indicate uptake by the biosphere.

3.4. Light Response (SiB3-SS, or Sunlit/Shaded)

[19] Increased sensitivity in model response to seasonal and diurnal variation in radiative forcing has been accomplished by explicitly resolving sunlit and shaded canopy fractions for energetics and photosynthetic processes [i.e., *de Pury and Farquhar*, 1997; *Wang and Leuning*, 1998; *Dai et al.*, 2004]. We modified the SiB two-stream canopy radiative transfer submodel [*Sellers*, 1985; *Sellers et al.*, 1996a] and canopy photosynthesis treatment [*Sellers et al.*, 1992] to accommodate sunlit and shaded canopy fractions, and coupled these treatments to the prognostic canopy air space utilized in SiB as outlined in *Baker et al.* [2003] and *Vidale and Stöckli* [2005].

[20] The model was spun up from saturated soil conditions for 15 model years using the above four formulations and three years of observed meteorological forcing (2001–2003).

4. Results and Discussion

[21] These four treatments were simulated individually and their performance was analyzed against observed fluxes of carbon, energy and moisture, although CO_2 flux is emphasized. All of these mechanisms were included in SiB3's model physics for a final simulation. These runs are shown in Figure 2. Monthly mean carbon flux from the
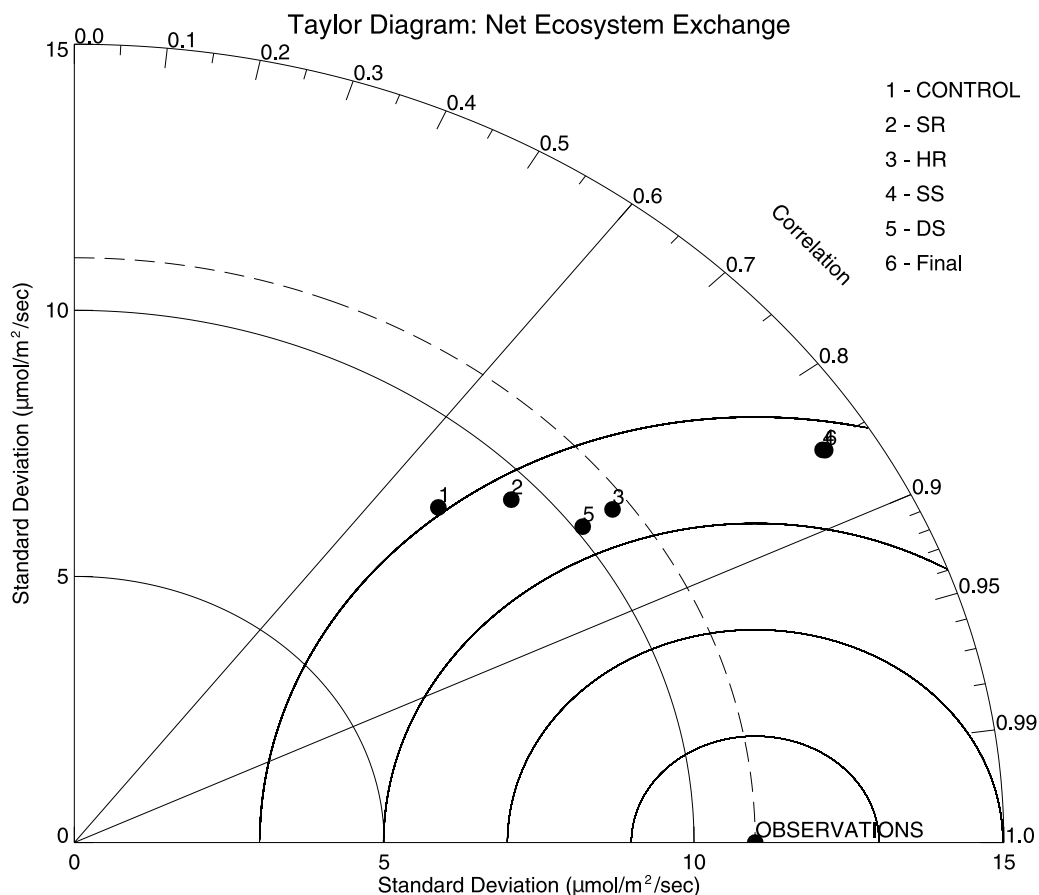
Figure 3. Taylor plot of 30-min modeled NEE against observed for years 2001–2003. Runs are identified as follows: (1) control run, (2) SiB3-SR, (3) SiB3-HR, (4) SiB3-SS, (5) SiB3-DS, and (6) combination.

SS run is similar to the results from the HR simulation. The effect of the sunlit/shaded (SS) run is seen in the short-term temporal response of CO_2 flux; these results will be addressed later, and are not shown in Figure 2.

[22] In the control simulation (Figure 1) with the unmodified code, respiration is almost constant throughout the year, while NPP decreases during the dry season (not shown). As mentioned previously, there is little response in heterotrophic respiration to drying soil, most likely due to the inappropriate value for optimum soil moisture for respiration. Any moisture response in respiration appears to be compensated for by a temperature response to slightly warming soils during the seasonal drought. The main driver of the annual NEE cycle is the dramatic decrease in NPP with decreasing soil moisture. Moisture storage in the soil is adequate to maintain photosynthesis through June, but by August NPP has shut down to less than half the value at maximum productivity in May and June. Photosynthesis does not recover completely until March or April, when the soil moisture has been recharged by rain. It is interesting to note that increasing the soil depth of the base case from 3.5 to 10 m has almost no effect on simulated fluxes. Near-surface soil layers, which contain the most roots, continue to dominate ecosystem behavior. These surface layers still desiccate quickly after rainfall ceases, so that the annual NEE cycle is almost indistinguishable from that shown in Figure 1.

[23] Relaxing the linkage between root distribution and stress postpones the change from uptake to efflux by 3 months (September versus July), but the general behavior of SiB3-SR (Figure 2a) is the same as the base case. Photosynthesis decreases as the soil desiccates and respiration is nearly constant through the entire year. In this case, the reservoir of available water in a 3.5 m deep soil is simply not sufficient to maintain ecosystem function through seasonal drought.

[24] In the hydraulic redistribution case (Figure 2b), the annual cycle of photosynthesis is almost uniform. Dry season stress, while still present, is minimal. However, heterotrophic respiration is also nearly constant in time, as opposed to observations that show a respiration decrease during seasonal drought [*Goulden et al.*, 2004]. The modeled respiration actually increases in the dry season in response to slightly warmer surface soil temperature as radiation increases with decreasing cloudiness. The annual NEE cycle, while much smaller in magnitude than in the control case, maintains the sign relationship between wet and dry seasons, which is inverted from the observed.

[25] The deep soil case, where we increase soil depth from 3.5 to 10 m and alter the respiration response to soil moisture, shows dramatic improvement over the control, SR
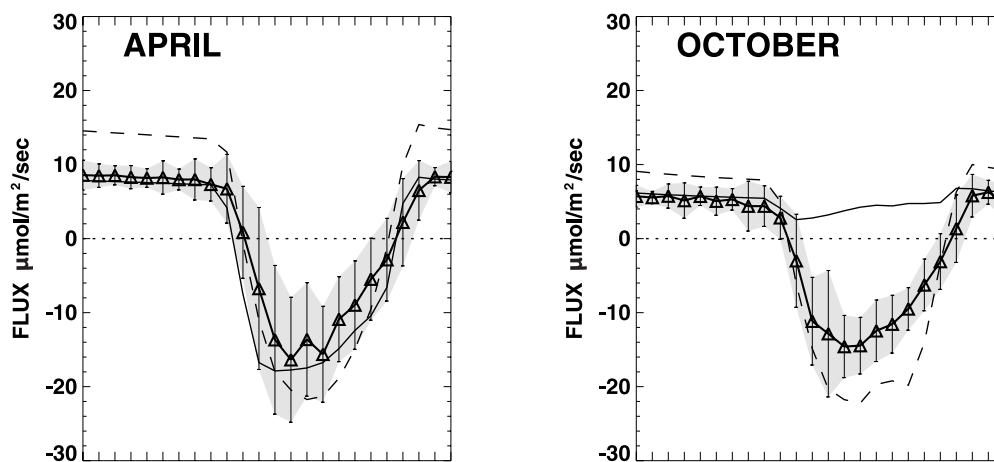
Figure 4. Monthly mean diurnal composited NEE for wet (April) and dry (October) months. Solid line with triangles is observed NEE, and shaded area represents ±1 standard deviation about the mean. Control run is shown as a thin solid line, and final simulation combining all mechanisms is shown as a dashed line.

and HR cases (Figure 2c). We have also included the relaxed dependence on root distribution in this case, to distinguish it from the base case with deep soil. SiB3-DS is the SiB3-RS case with deeper soil and adjusted respiration response. NPP shows a maximum during the early stages of the dry season, in response to favorable light and soil moisture conditions. Heterotrophic respiration decreases as surface soil dries out. The surface soil has the largest root density, so under optimum conditions transpiration will remove water from the surface layers first. Radiative forcing at the ground surface is minimal beneath the closed canopy, but soil surface evaporation plays a small role. Without hydraulic redistribution to recharge the surface layers, the shallow soil becomes increasingly desiccated through the dry season, and transpiration load is transferred to the deeper layers in the soil. This combination of photosynthetic and respiration behavior has the effect of reversing the previously modeled NEE cycle, to the point where the sign of the annual cycle is now consistent with observations. There is efflux during the wet season, and uptake during seasonal drought. The modeled NEE now has monthly mean magnitude comparable to observed for both segments of the cycle. Mean uptake of carbon begins early in SiB3-DS (July versus August), but the sign of all other months are consistent with observed. This represents a large positive departure from previous model results.

[26] The differences between the deep soil (SiB3-DS) and final simulation (Figure 2d, representing a combination of the SiB3-HR, SiB3-SS and SiB3-DS runs) are subtle on the monthly mean scale. The annual cycle remains consistent with observed, with the difference that July is now a month of efflux and January a month of uptake in the model results. The amplitude of the annual cycle of NEE is decreased by approximately 15% from the SiB3-DS to the SiB3-final run, while the amplitudes of the NPP and respiration annual cycles are both decreased by approximately 25%. This result is not inconsistent, since the timing of the variability is not temporally uniform. In the SiB3-DS run, the temporal peaks of respiration and photosynthesis are more pronounced, while in the final run the simulation

produces a more stable or uniform behavior between wet and dry seasons. The end result, monthly mean NEE, is similar between the SiB3-DS and final runs, but the mechanisms have been modified.

[27] The sensitivity of SiB3 to the various mechanisms is shown in a Taylor plot [*Taylor*, 2001] in Figure 3. Correlation coefficient is improved when compared to the control run in all simulations, but the largest correlation occurs in the SiB3-SS and final runs, which are virtually identical at a correlation coefficient of 0.85. It is interesting to note that although the correlation to the observations is high for SiB3-SS, the annual cycle was still inverted. In SiB3, adjusting the light response had a large impact on the diurnal scale, but not on monthly mean NEE. By increasing SiB3 response to light, we improve the correlation to the high-frequency observations. The variability of all simulations that did not include light response was smaller than observed, while the variability of the two simulations that included light response (SiB3-SS and final) were significantly larger than observed. By including sunlit and shaded canopy fractions in SiB3, GPP was increased by 25–30%. To maintain annual carbon balance, there was an attendant increase in heterotrophic respiration [*Denning et al.*, 1996]. Therefore, adjusting the light response increased the amplitude of the diurnal cycle of NEE, but decreased the annual cycle of monthly mean NEE. Figure 4 shows monthly mean diurnal composites of NEE for April and October, aggregated over all years. For both wet and dry seasons the final run has a larger amplitude than the control run. However, the final run also simulates uptake during October (dry season) where the control run canopy is almost completely inactive. The shape of the diurnal cycle is closer to observed in the final run. This can be seen both in the larger correlation in the Taylor plot, and visually in Figure 4 as well.

[28] However, SiB3 model physics do not include all details of local phenology, such as the genetically induced cycles of litterfall and wood increment as noted by *Goulden et al.* [2004]. SiB3 also maintains a constant annual leaf area index (LAI) for broadleaf evergreen forests. LAI and, more
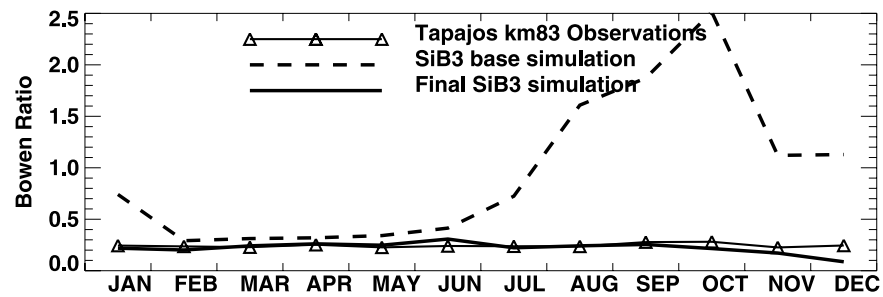
Figure 5. Monthly mean Bowen ratio at Tapajos National Forest km83 site, years 2001–2003. Observations are shown as a solid line with triangular symbols. Control simulation is a dashed line, and final simulation is a solid line.

importantly, fraction of photosynthetically active radiation (fPAR) are obtained from satellite observations; water vapor and cloud contamination of satellite observations can induce errors in surface fluxes in SiB3 [*Los et al.*, 2000]. *Huete et al.* [2006] and *Saleska et al.* [2007] attribute part of the green-up in the Amazon Basin during the dry season to increased LAI. This feature will not be reflected in SiB3 simulations, and suggests that we may not currently have the ability to capture completely all mechanisms that effect biophysical function in the region.

[29] It is well-known that eddy covariance instruments do not close energy budgets [i.e., *Mahrt*, 1998; *Wilson et al.*, 2002]. The sum of latent, sensible, and ground heat fluxes has a deficit generally on the order of 10–30% less than incoming radiation [*Twine et al.*, 2000]. This closure problem exists with carbon flux as well [*Aranibar et al.*, 2006], and there are additional issues of underrepresentation of nocturnal CO_2 efflux [*Eugster and Siegrist*, 2000; *Lee*, 1998] though the site researchers at km83 made a strong effort to correct for this [*Miller et al.*, 2004]. Therefore, it is reasonable to assume that the magnitude of the observed NEE is smaller than reality. For this reason, a model simulation that has variability smaller than or equal to the observed, as in the case of the control, SiB3-HR and SiB3-DS runs (Figure 3) almost surely has magnitude that is too small. Following this line of reasoning, we might expect that a model simulation with variability exceeding the observed is reasonable, but determining the optimum excess is difficult owing to multiple processes affecting both observations and model results. In this case, we see standard deviation of the SiB3 runs with the sunlit/shaded canopy simulation (and in the final run) that is 30% larger than observed. Intuitively this seems large. However, a detailed investigation of observed carbon flux closure is beyond the scope of this paper; we will accept the increase in correlation coefficient and larger-than-observed variability as positive results.

[30] Finally, although the emphasis here has been on CO_2 flux, the large fraction of total water flux occurring as transpiration (80–85% in SiB3 simulations) tightly couples fluxes of latent and sensible heat to vegetation behavior. Modeled and observed values of Bowen ratio are shown in Figure 5. In the unmodified case, Bowen ratio becomes large during the dry season as transpiration wanes owing to soil water stress and attendant stomatal closure. The Bowen ratio in the final run is almost constant throughout the year, as is the observed. The magnitude of the individual fluxes

(latent and sensible heat; not shown) is similar to observed in the final run as well.

5. Conclusions

[31] We modified the model physics in the simple biosphere model (SiB3) to include mechanisms that allow broadleaf evergreen forests in tropical Amazonia to maintain biophysical function through seasonal drought. This changed model response from an inverted annual NEE cycle to one that has the same general behavior as observed eddy covariance fluxes. The mechanisms we included are deeper soils and a modification of the soil moisture respiration optimum value, modified root water uptake function, hydraulic redistribution, and light response. We found that each process, individually incorporated into SiB3, was not sufficient to change the sign of the annual NEE cycle to match observations.

[32] Increasing soil depth to 10 m and allowing roots to access this entire reservoir had the effect of removing stress from vegetation during the dry season, although a similar response was obtained with hydraulic redistribution incorporated into SiB3. In each case, the respiration response was critical to the annual NEE. By changing the soil moisture value most favorable to respiration from 60% to 75% of saturation, we were able to induce a reduction in near-surface root respiration in the SiB3-DS case like that observed in the field [*Goulden et al.*, 2004], resulting in net carbon uptake during the drier months. In the SiB3-HR case, hydraulic redistribution kept near-surface soil layers moist, and there was no respiration response to drying soil. In fact, in the SiB3-HR case respiration actually increased in the dry season owing to slightly warmer temperatures.

[33] When canopy response was modeled explicitly for sunlit and shaded fractions (SiB3-SS), the response in the monthly mean was minimal. The largest change was in the magnitude and shape of the diurnal cycle.

[34] The above points underscore the concept of equifinality, or multiple paths to a single solution in a model. For example, observed NEE reveals vegetation uptake of carbon in the dry season, and efflux when rain is plentiful. In the model, we can reproduce this result two ways: (1) photosynthesis is constant annually, and respiration decreases in the dry season as surface litter and soil desiccate, and (2) annual respiration is constant, and photosynthesis increases in the dry season in response to higher light levels. Observed NEE does not partition the individual

contribution of photosynthesis and respiratory components, but it is intuitive to believe that the actual canopy response is a combination of choices 1 and 2. It is desirable to quantify the relative response of each, but that is likely to be variable in space and time.

[35] As pointed out by *Franks et al.* [1997], eddy covariance fluxes by themselves are insufficient to provide a robust calibration of process-based biophysical models. Therefore, model simulations must be confronted with observational data from multiple sources to prevent modelers from getting "the right answer for the wrong reason." Open lines of communication between the observational and modeling communities are critical to this effort.

[36] This research represents initial success in simulating the correct sign in the annual NEE cycle at an single location in the Amazon Basin. We have done so by identifying several mechanisms identified in the literature as having a bearing on the observed behavior in the region, specifically (1) the ability of roots to access moisture in deep soil layers, (2) the ability of hydraulic redistribution of soil moisture by roots to both make water available to roots and to more efficiently use the pore space in the soil to store water, and (3) the ability of the vegetation to utilize increased light during the dry season, when more incoming radiation is available. By incorporating these mechanisms into SiB3 we are able to obtain an annual cycle of NEE that matches the observed, specifically uptake of carbon during the dry season and efflux during the wet months. We have shown the average results for three years of simulations (2001–2003), as the initial goal is to be able to reproduce the general response of the vegetation in the region. As our understanding of the biophysical processes increases, we will be in a position to investigate variability about the mean. We have shown that we can obtain the right sign for a single station. The next step is to reproduce the analysis across moisture and vegetation gradients across the Amazon Basin.

References

Adler, R. F., et al. (2003), The version 2 Global Precipitation Climatology Project (GPCP) monthly precipitation analysis (1979-present), *J. Hydrometeorol.*, 4, 1147–1167.

Andreae, M. O., et al. (2002), Biogeochemical cycling of carbon, water, energy, trace gases, and aerosols in Amazonia: The LBA-EUSTACH experiments, *J. Geophys. Res.*, 107(D20), 8066, doi:10.1029/2001JD000524.

Aranibar, J. N., J. A. Berry, W. J. Riley, D. E. Patakis, B. E. Law, and J. R. Ehleringer (2006), Combining meteorology, eddy fluxes, isotope measurements, and modeling to understand environmental controls of carbon isotope discrimination at the canopy scale, *Global Change Biol.*, 12, 710–730.

Avissar, R., and D. Werth (2004), Global hydroclimatological teleconnections resulting from tropical deforestation, *J. Hydrometeorol.*, 6, 134–145.

Avissar, R., P. L. Silva Dias, M. A. F. Silva Dias, and C. Nobre (2002), The Large-Scale Biosphere-Atmosphere Experiment in Amazonia (LBA): Insights and future research needs, *J. Geophys. Res.*, 107(D20), 8086, doi:10.1029/2002JD002704.

Baker, I. T., A. S. Denning, N. Hanan, L. Prihodko, P.-L. Vidale, K. Davis, and P. Bakwin (2003), Simulated and observed fluxes of sensible and latent heat and CO_2 at the WLEF-TV Tower using SiB2.5, *Global Change Biol.*, 9, 1262–1277.

Baker, I. T., A. S. Denning, L. Prihodko, K. Schaefer, J. A. Berry, G. J. Collatz, N. S. Suits, R. Stöckli, A. Philpott, and O. Leonard (2007), Global net ecosystem exchange (NEE) of CO_2, http://www.daac.ornl.gov, Oak Ridge Natl. Lab. Distrib. Active Archive Cent., Oak Ridge, Tenn.

Bousquet, P., P. Peylin, P. Ciais, C. Le Quere, P. Friedlingstein, and P. P. Tans (2000), Regional changes in carbon dioxide fluxes of land and oceans since 1980, *Science*, 290, 1342–1346.

Collatz, G. J., J. T. Ball, C. Grivet, and J. A. Berry (1991), Physiological and environmental regulation of stomatal conductance, photosynthesis and transpiration: A model that includes a laminar boundary layer, *Agric. For. Meteorol.*, 54, 107–136.

Collatz, G. J., M. Ribas-Carbo, and J. A. Berry (1992), Coupled photosynthesis-stomatal conductance model for leaves of C4 plants, *Aust. J. Plant Physiol.*, 19(5), 519–538.

Cox, P. M., R. A. Betts, C. D. Jones, S. A. Spall, and I. J. Totterdell (2000), Acceleration of global warming due to carbon-cycle feedbacks in a coupled climate model, *Nature*, 408, 184–187.

Dai, Y., et al. (2003), The common land model (CLM), *Bull. Am. Meteorol. Soc.*, 84, 1013–1023.

Dai, Y., R. E. Dickinson, and Y.-P. Wang (2004), A two-big-leaf model for canopy temperaure, photosynthesis, and stomatal conductance, *J. Clim.*, 17, 2281–2299.

da Rocha, H. R., M. L. Goulden, S. D. Miller, M. C. Menton, L. D. V. O. Pinto, H. C. de Frietas, and A. M. e Silva Figueira (2004), Seasonality of water and heat fluxes over a tropical forest in eastern Amazonia, *Ecol. Appl.*, 14(4), supplement, S22–S32.

Denning, A. S., G. J. Collatz, C. Zhang, D. A. Randall, J. A. Berry, P. J. Sellers, G. D. Colello, and D. A. Dazlich (1996), Simulations of terrestrial carbon metabolism and atmospheric CO_2 in a general circulation model. Part 1: Surface carbon fluxes, *Tellus, Ser. B*, 48, 521–542.

de Pury, D. G. G., and G. D. Farquhar (1997), Simple scaling of photosynthesis from leaves to canopies without the errors of big-leaf models, *Plant Cell Environ.*, 20, 537–557.

Eugster, W., and F. Siegrist (2000), The influence of nocturnal CO_2 advection on CO_2 flux measurements, *Basic Appl. Ecol.*, 1, 177–188.

Farquhar, G. D., S. von Caemmerer, and J. A. Berry (1980), A biochemical model of photosynthetic CO_2 assimilation in leaves of C3 species, *Planta*, 149, 78–90.

Franks, S. W., K. J. Beven, P. F. Quinn, and I. R. Wright (1997), On the sensitivity of soil-vegetation-atmosphere transfer (SVAT) Schemes: Equifinality and the problem of robust calibration, *Agric. For. Meteorol.*, 86, 63–75.

Friedlingstein, P. F., L. Bopp, P. Ciais, J.-L. Dufresne, L. Fairhead, H. LeTreut, P. Monfray, and J. Orr (2001), Positive feedback between future climate change and the carbon cycle, *Geophys. Res. Lett.*, 28(8), 1543–1546.

Goulden, M. L., S. D. Miller, H. R. da Rocha, M. C. Menton, H. C. de Freitas, A. M. e Silva Figueira, and C. A. D. de Sousa (2004), Diel and seasonal patterns of tropical forest CO_2 exchange, *Ecol. Appl.*, 14(4), supplement, S42–S54.

Gurney, K. R., et al. (2002), Towards robust regional estimates of CO_2 sources and sinks using atmospheric transport models, *Nature*, 415, 626–629.

Hanan, N. P., J. A. Berry, S. B. Verma, E. A. Walter-Shea, A. E. Suyker, G. G. Burba, and A. S. Denning (2005), Testing a model of CO_2, water and energy exchange in Great Plains tallgrass prairie and wheat ecosystems, *Agric. For. Meteorol.*, 131, 162–179.

Houghton, R. A., D. S. Skole, C. A. Nobre, J. A. Hackler, K. T. Lawrence, and W. H. Chomentowski (2000), Annual fluxes of carbon from deforestation and regrowth in the Brazillian Amazon, *Nature*, 403, 301–304.

Houghton, R. A., K. T. Lawrence, J. L. Hackler, and S. Brown (2001), The spatial distribution of forest biomass in the Brazilian Amazon: A comparison of estimates, *Global Change Biol.*, 7, 731–746.

Huete, A. R., K. Didan, Y. E. Shimabukuro, P. Ratana, S. R. Salexska, L. R. Hutyra, W. Yang, R. R. Nemani, and R. Myneni (2006), Amazon rainforests green-up with sunlight in dry season, *Geophys. Res. Lett.*, 33, L06405, doi:10.1029/2005GL025583.

Ichii, K., H. Hashimoto, M. A. White, C. Potter, L. R. Hutyra, A. R. Huete, R. B. Myneni, and R. R. Nemani (2007), Constraining rooting depths in tropical rainforests using satellite data and ecosystem modeling for accurate simulation of gross primary production seasonality, *Global Change Biol.*, 13, 67–77, doi:10.1111/j.1365-2486.2006.01277.x.

Jackson, R. B., J. Canadell, J. R. Ehleringer, H. A. Mooney, O. E. Sala, and E. D. Schulze (1996), A global analysis of root distributions for terrestrial biomes, *Oecologia*, 108, 389–411.

Jipp, P. H., D. C. Nepstad, D. K. Cassel, and C. R. de Carvalho (1998), Deep soil moisture storage and transpiration in forests and pastures of seasonally-dry Amazonia, *Clim. Change*, 39, 395–412.

Keller, M., et al. (2004), Ecological research in the large-scale biosphere-atmosphere experiment in Amazonia: Early results, *Ecol. Appl.*, 14(4), supplement, S3–S16.

Kleidon, A., and M. Heimann (1999), Deep-rooted vegetation, Amazonian deforestation and climate: Results from a modelling study, *Global Ecol. Biogeogr.*, 8(5), 397–405.

Lee, J.-E., R. S. Oliveira, T. E. Dawson, and I. Fung (2005), Root functioning modifies seasonal climate, *Proc. Natl. Acad. Sci. U. S. A.*, 102(49), 17,576–17,581.

Lee, X. (1998), On micrometeorological observations of surface-air exchange over tall vegetation, *Agric. For. Meteorol.*, 91, 39–49.

Los, S. O., G. J. Collatz, P. J. Sellers, C. M. Malmstrom, N. H. Pollack, R. S. DeFries, L. Bounoua, M. T. Parris, C. J. Tucker, and D. A. Dazlich (2000), A global 9-year biophysical land surface dataset from NOAA AVHRR data, *J. Hydrometeorol.*, 1, 183–199.

Magrin, G., C. Gay Garcia, D. Cruz Choque, J. C. Giménez, A. R. Moreno, G. J. Nagy, C. Nobre, and A. Villamizar (2007), Latin America, in *Climate Change 2007: Impacts, Adaptation and Vulnerability. Contribution of Working Group II to the Fourth Assessment Report of the Intergovernmental Panel on Climate Change*, edited by M. L. Parry et al., pp. 581–615, Cambridge Univ. Press, Cambridge, U.K.

Mahrt, L. (1998), Flux sampling errors for aircraft and towers, *J. Atmos. Oceanic Technol.*, 15(2), 416–429.

Marengo, J. A., and C. A. Nobre (2001), General Characteristics and Variability of Climate in the Amazon Basin and Its Links to the Global Climate System, in *The Biogeochemistry of the Amazon Basin*, edited by M. E. McClain, R. L. Victoria, and J. E. Richey, Oxford Univ. Press, Oxford, U.K.

Miller, S. D., M. L. Goulden, M. C. Menton, H. R. da Rocha, H. C. de Freitas, A. M. E. S. Figueira, and C. A. D. de Sousa (2004), Biometric and micrometeorological measurements of tropical forest carbon balance, *Ecol. Appl.*, 14(4), supplement, S114–S126.

Nepstad, D. C., C. R. de Carvlho, E. A. Davidson, P. H. Jipp, P. A. Lefebvre, G. H. Negreiros, E. D. da Silva, T. A. Stone, S. E. Trumbore, and S. Vieira (1994), The role of deep roots in the hydrological and carbon cycles of Amazonian forest and pastures, *Nature*, 372, 666–669.

Nobre, C. A., P. J. Sellers, and J. Shukla (1991), Amazonian deforestation and regional climate change, *J. Clim.*, 4, 957–988.

Oliveira, R. S., T. E. Dawson, S. S. O. Burgess, and D. C. Nepstad (2005), Hydraulic redistribution in three Amazonian trees, *Oecologia*, 145, 354–363.

Raich, J. W., E. B. Rastetter, J. M. Melilllo, D. W. Kicklighter, P. A. Steudler, B. J. Peterson, A. L. Grace, B. Moore III, and C. J. Vorosmarty (1991), Potential net primary productivity in South America: Application of a global model, *Ecol. Appl.*, 1(4), 399–429.

Randall, D. A., et al. (1996), A revised land surface parameterization (SiB2) for GCMs. Part III: The greening of the Colorado State University General Circulation Model, *J. Clim.*, 9, 738–763.

Romero-Saltos, H., L. S. L. Sternberg, M. Z. Moreira, and D. C. Nepstad (2005), Rainfall exclusion in an eastern Amazonian forest alters soil water movement and depth of water uptake, *Am. J. Bot.*, 92(3), 443–455.

Ryel, R. J., M. M. Caldwell, C. K. Yoder, D. Or, and A. J. Leffler (2002), Hydraulic redistribution in a stand of Artemisia tridentata: Evaluation of benefits to transpiration assessed with a simulation model, *Oecologia*, 130, 173–184.

Salati, E., and P. B. Vose (1984), Amazon Basin: A system in equilibrium, *Science*, 225, 129–138.

Saleska, S. R., et al. (2003), Carbon in Amazon forests: Unexpected seasonal fluxes and disturbance-induced losses, *Science*, 302, 1554–1557.

Saleska, S. R., K. Didan, A. R. Huete, and H. R. da Rocha (2007), Amazon forests green-up during 2005 drought, *Science*, 318, 612, doi:10.1126/science.1146663.

Sellers, P. J. (1985), Canopy reflectance, photosynthesis and transpiration, *Int. J. Remote Sens.*, 6(8), 1335–1372.

Sellers, P. J., Y. Mintz, Y. C. Sud, and A. Dalcher (1986), A simple biosphere model (SiB) for use within general circulation models, *J. Atmos. Sci.*, 43(6), 505–531.

Sellers, P. J., J. A. Berry, G. J. Collatz, C. B. Field, and F. G. Hall (1992), Canopy reflectance, photosynthesis, and transpiration. III. A reanalysis using improved leaf models and a new canopy integration scheme, *Remote Sens. Environ.*, 42, 216–1878.

Sellers, P. J., D. A. Randall, G. J. Collatz, J. A. Berry, C. B. Field, D. A. Dazlich, C. Zhang, G. D. Colello, and L. Bounoua (1996a), A revised land surface parameterization (SiB2) for atmospheric GCMs. Part I: Model formulation, *J. Clim.*, 9, 676–705.

Sellers, P. J., S. O. Los, C. J. Tucker, C. O. Justice, D. A. Dazlich, G. J. Collatz, and D. A. Randall (1996b), A revised land surface parameterization (SiB2) for atmospheric GCMs. Part II: The generation of global fields of terrestrial biophysical parameters from satellite data, *J. Clim.*, 9, 706–737.

Silver, W. L., J. Neff, M. McGroddy, E. Veldkamp, M. Keller, and R. Cosme (2000), Effects of soil temperature on belowground carbon and nutrient storage in a lowland Amazonian forest ecosystem, *Ecosystems*, 3, 193–209.

Stephens, B. B., et al. (2007), Weak northern and strong tropical land carbon uptake from vertical profiles of atmospheric CO_2, *Science*, 316, 1732–1735.

Taylor, K. E. (2001), Summarizing multiple aspects of model performance in a single diagram, *J. Geophys. Res.*, 106(D7), 7183–7192.

Tucker, C. J., J. E. Pinzon, M. E. Brown, D. A. Slayback, E. W. Pak, R. Mahoney, E. F. Vermote, and N. El Saleous (2005), An extended AVHRR 8-km NDVI dataset compatible with MODIS and SPOT vegetation NDVI data, *Int. J. Remote Sens.*, 26(20), 4485–4498.

Twine, T. E., W. P. Kustas, J. M. Norman, D. R. Cook, P. R. Houser, T. P. Meyers, J. H. Prueger, P. J. Starks, and M. L. Wesely (2000), Correcting eddy-covariance flux underestimates over a grassland, *Agric. For. Meteorol.*, 103, 279–300.

Vidale, P. L., and R. Stöckli (2005), Prognostic canopy air solutions for land surface exchanges, *Theor. Appl. Climatol.*, 80, 245–257.

Wang, Y.-P., and R. Leuning (1998), A two-leaf model for canopy conductance, photosynthesis and partitioning of available energy I: Model description and comparison with a multi-layered model, *Agric. For. Meteorol.*, 91, 89–111.

Wilson, K., et al. (2002), Energy balance closure at FLUXNET sites, *Agric. For. Meteorol.*, 113, 223–243.

Zeng, N., A. Mariotti, and P. Wetzel (2005), Terrestrial mechanisms of interannual CO_2 variability, *Global Biogeochem. Cycles*, 19, GB1016, doi:10.1029/2004GB002273.

―――――――――――

I. T. Baker and A. S. Denning, Atmospheric Science Department, Colorado State University, 1371 Campus Delivery, Fort Collins, CO 80523-1371, USA. (baker@atmos.colostate.edu; denning@atmos.colostate.edu)

H. da Rocha, Instituto de Astronomica, Geofisica e Ciencias Atmosfericas, Universidade de São Paulo, Rua do Matao 1226, São Paulo SP 05508-090, Brazil. (humberto@model.iag.usp.br)

M. Goulden, University of California, Irvine, 3319 Croul Hall, Irvine, CA 92697-3100, USA. (mgoulden@uci.edu)

S. Miller, Atmospheric Sciences Research Center, State University of New York at Albany, 251 Fuller Road, Albany, NY 12203, USA. (smiller@albany.edu)

L. Prihodko, Natural Resources Ecology Laboratory, Colorado State University, 1499 Campus Delivery, Fort Collins, CO 80523-1499, USA. (lara@nrel.colostate.edu)